

Relationship between Sequence Distribution and Thermal Properties of the Transesterification Product between Poly(ethylene terephthalate) and Poly(butylene terephthalate)

Hironori Matsuda and Tetsuo Asakura*

Department of Biotechnology, Tokyo University of Agriculture and Technology,
Koganei, Tokyo 184-8588, Japan

Bunsow Nagasaka

Material Analysis Research Laboratories, Teijin Ltd., Hino, Tokyo 191-8512, Japan

Kazuhiko Sato

Innovation Research Institute, Teijin Ltd., Iwakuni, Yamaguchi 740-0014, Japan

Received March 15, 2004; Revised Manuscript Received April 19, 2004

ABSTRACT: The relationship between the number-average sequence length and the melting temperature of the block copolyesters prepared by quench after the transesterification reaction between poly(ethylene terephthalate) and poly(butylene terephthalate) was reported. The number-average sequence length was determined by the triad sequence analysis in a solvent system of *o*-chlorophenol/deuterated chloroform mixture (75/25 v/v) at 80 °C using 600 MHz ¹H NMR. The melting temperature was observed using a differential scanning calorimeter. The linear correlation between the melting temperature and the inverse of the number-average sequence length was observed for the transesterification products with composition of PET/PBT from 20/80 to 80/20 mol %. This correlation was confirmed by the measurement of the long period using small-angle X-ray scattering. For the transesterification products obtained under definite conditions such as the quench after the transesterification reaction, it was confirmed that the number-average sequence length measured by NMR can be approximately used instead of the lamellae thickness in Gibbs–Thomson equation that has been well-known as the relationship between the melting temperature and the lamellae thickness. The decrease in the ratio of the relative peak area of the methylene carbon of the butylene glycol and ethylene glycol units, $I_{\text{PBT}}/I_{\text{PET}}$, in the solid-state ¹³C NMR spectra was observed as the progress of the transesterification. This seems due to change in the local motion of each segment reflecting the decrease of the crystalline size.

Introduction

Polyester is used in large quantities in the textile industry and also in the manufacture of electronic tapes, food packaging, and beverage containers. To overcome some drawbacks of polyesters, copolymerization has been performed. Copolyesters can be synthesized by transesterification in the polymer blends. The degree of sequence randomness of copolyester can be easily controlled with the conditions of the transesterification reaction. The transesterification method is important to the industry because the thermal and mechanical properties of a copolyester are related to the degree of sequence randomness.

A large number of sequence analyses of copolyesters have been reported using nuclear magnetic resonance (NMR).^{1–4} Recent development of NMR apparatus and its technique makes possible to obtain the detailed sequence information for the copolymers. In our previous paper,⁵ we reported the longer sequence analysis of the transesterification products obtained from poly(ethylene terephthalate) (PET) and poly(butylene terephthalate) (PBT) by the selection of the suitable solvent and temperature and by use of a high-field NMR instrument. It seems important to clarify the relationship between the sequence information obtained by NMR and the melting temperature of the block copolyesters obtained by the transesterification reaction be-

tween PET and PBT. Several theories on the melting temperature of the copolymers have been reported.^{6–14} For example, the melting temperature in a completely random A/B-copolymer system is expressed as a function of the copolymer composition or sequence distribution as proposed by Flory⁶ or Brau⁷ et al. On the other hand, the Gibbs–Thomson equation on the melting temperature of a polymer has been well-known¹⁵ and applied.^{16,17} The Gibbs–Thomson equation expresses the relationship between the melting temperature and the lamellae thickness that is usually measured by transmission electron microscopy (TEM). Many studies, however, have been reported on the relationship between the monomer composition^{19–28} rather than sequence distribution¹⁸ and the melting temperature for the block copolyesters obtained by the transesterification reaction. There is limited report on the correlation between the primary structural information, such as sequence distribution, and the tertiary structural information, such as the lamellae thickness or crystalline size, for the block copolyesters prepared by transesterification.

In this paper, we will discuss the relationship between the sequence distribution and the melting temperature by modification of the Gibbs–Thomson equation for the block copolyester obtained by the transesterification reaction between PET and PBT. By the analyses using ¹H NMR, differential scanning calorimetry (DSC), and small-angle X-ray scattering (SAXS), the linear correlation between the inverse of the number-average se-

* To whom correspondence should be addressed. E-mail: asakura@cc.tuat.ac.jp.

quence length and the melting temperature of the block copolyester obtained by quench after the transesterification reaction between PET and PBT will be pointed out. That is, it was confirmed that the number-average sequence length obtained by NMR can be approximately used instead of the lamellae thickness in the Gibbs–Thomson equation for the transesterification product. This indicates that the tertiary structure, the lamellae thickness or crystalline size, of the transesterification products correlates with the primary structure, sequence distribution, and the crystallization behavior is influenced by the sequence distribution. Therefore, it seems that the number-average sequence length obtained by NMR is useful for the prediction of T_m value or for the index of T_m control for the block copolymers obtained by the transesterification reaction. Here, the structure of the transesterification products was also analyzed using high-resolution solid-state ^{13}C NMR.

Experimental Section

Material. The blend of PET and PBT, of which unit ratio was 40 and 60 mol %, respectively, was prepared by dissolving two polymers in a hexafluoro-2-propanol. The polymer solution was then poured into a large excess of acetone. The precipitated polymer was filtered off and then dried in a vacuum at 50 °C for 24 h. Other blends of PET and PBT, blend ratios 20 and 80, 60 and 40, and 80 and 20 mol %, were also prepared. Transesterification products were prepared by the following. Heat treatment of the blend of PET and PBT was performed on a TA Instruments 2920 differential scanning calorimeter under dry nitrogen atmosphere. Samples were heated from room temperature to 300 °C with heating rate of 50 K min⁻¹, maintained at that temperature for various time intervals, and quenched into ice/water. Densities of the transesterification products were measured in a cyclohexane/tetrachloroethane density gradient column at 25 °C. The triad fractions and the number average-sequence lengths of the transesterification products between PET and PBT were analyzed in a solvent system of *o*-chlorophenol/deuterated chloroform mixture (75/25 v/v) at 80 °C using a JEOL α-600 spectrometer operating at 600 MHz ^1H NMR as reported in our previous paper.⁵

SAXS Measurements. Small-angle X-ray scattering (SAXS) measurements were performed on a setup consisting of a rotating anode X-ray source (Rigaku RU-200B, $\lambda(\text{Cu K}\alpha) = 0.154$ nm), 45 kV and 70 mA. The incident X-ray beam was monochromatized and focused with a Osmic's confocal mirror, and a set of three pinhole collimators were used. The scattered patterns were detected by an imaging plate (IP) with 120 × 120 mm² area (50 μm resolution). The sample to detector distance was 720 mm. A vacuum chamber was placed between the sample and IP to reduce air scattering and absorption.

DSC Measurements. DSC measurements were conducted using a TA Instruments 2920 differential scanning calorimeter instrument under dry nitrogen atmosphere. Samples were heated from room temperature to 300 °C with heating rate of 20 K min⁻¹.

Solid-State ^{13}C NMR Measurements. High-resolution solid-state ^{13}C NMR spectra were recorded by using a Bruker DSM300wb spectrometer operating at 75.5 MHz equipped with cross-polarization magic-angle sample spinning (CPMAS) accessories. CPMAS NMR spectra were measured at room temperature with 1 ms contact time, 5 s recycle delay, and 30 kHz spectral width, with high-power dipolar decoupling of ca. 74 kHz and MAS at 6.5 kHz. Chemical shifts were calibrated indirectly with the methyl resonance of solid hexamethylbenzene (17.6 ppm relative to tetramethylsilane). A series of cross-polarization experiments with varying contact times between 0.02 and 20 ms have been also performed.

Results and Discussion

Sequence Analysis Using ^1H NMR. The 600 MHz ^1H NMR spectra of the transesterification products

obtained by quench after the transesterification reaction between PET and PBT were measured in *o*-chlorophenol/deuterated chloroform mixture (75/25 v/v) at 80 °C upon the decoupling of the nonalcoholic methylene protons of the butylene glycol units. The expanded spectrum of the alcoholic CH₂ proton region together with the assignment is shown in Figure 1. The assignment was performed in our previous paper.⁵ The sequence distributions of several transesterification products between PET and PBT, the blend ratio is 40 and 60 mol %, respectively, were analyzed. On the basis of the observed relative peak area, triad molar fractions centered on glycol units and the number-average sequence length were determined as listed in Table 1.⁵

Thermal Properties. Figure 2 shows the DSC heating thermograms of the transesterification products between PET and PBT. The peaks were broadened with increasing the transesterification reaction time. This broadening results from wide distribution of the crystal size caused by the heterogeneity of the sequence with increasing of the transesterification reaction. The shoulders in the curves in Figure 2a,b result from the partial heterogeneity during the transesterification reaction under nonstirring conditions of this experiment. The melting temperatures of the samples were determined from the tops of the main peaks in Figure 2 and are listed in Table 2. The melting temperature depression was observed with the increase of transesterification reaction time.

The melting temperature in a completely random A/B copolymer system is expressed as a function of the copolymer composition (X). For example, when the sequences of A units in the random copolymer can be crystallized and B units are completely excluded from the crystals, the melting temperature proposed by Flory⁶ is expressed by the following equation:

$$1/T_m - 1/T_m^\circ = -(R/\Delta H_m) \ln X_A \quad (1)$$

Here T_m and T_m° are the equilibrium melting temperatures of a random copolymer of molar fraction X_A and the corresponding homopolymer, respectively. ΔH_m is the heat of fusion of a homopolymer, and R is the gas constant. Taking into account the effect of the sequence length of crystallizable units which can be crystallized only when their length corresponds to the crystal thickness, a modified exclusion theory for a random A/B copolymer system as proposed by Baur⁷ is expressed by the following equation:

$$1/T_m - 1/T_m^\circ = -(R/\Delta H_m) \ln(X_A - 1/L) \quad (2)$$

Here L is the number-average sequence length of crystallizable units, given by $[2X_A(1 - X_A)]^{-1}$ for a random copolymer system.

The cocrystallization behavior can be divided into three types, depending on the chemical structure and the crystallizability of the A and B monomer units:²²

(i) Crystallization of A or B units takes place either in an A-polymer or B-polymer crystal with complete rejection of the monomer units from the crystals.

(ii) A units can crystallize with complete rejection of the B units from the crystal, whereas B units can cocrystallize with incorporation of A units to some extent, depending on the copolymer composition.

(iii) A and B units can cocrystallize into a single-crystal structure over the full range of copolymer composition.

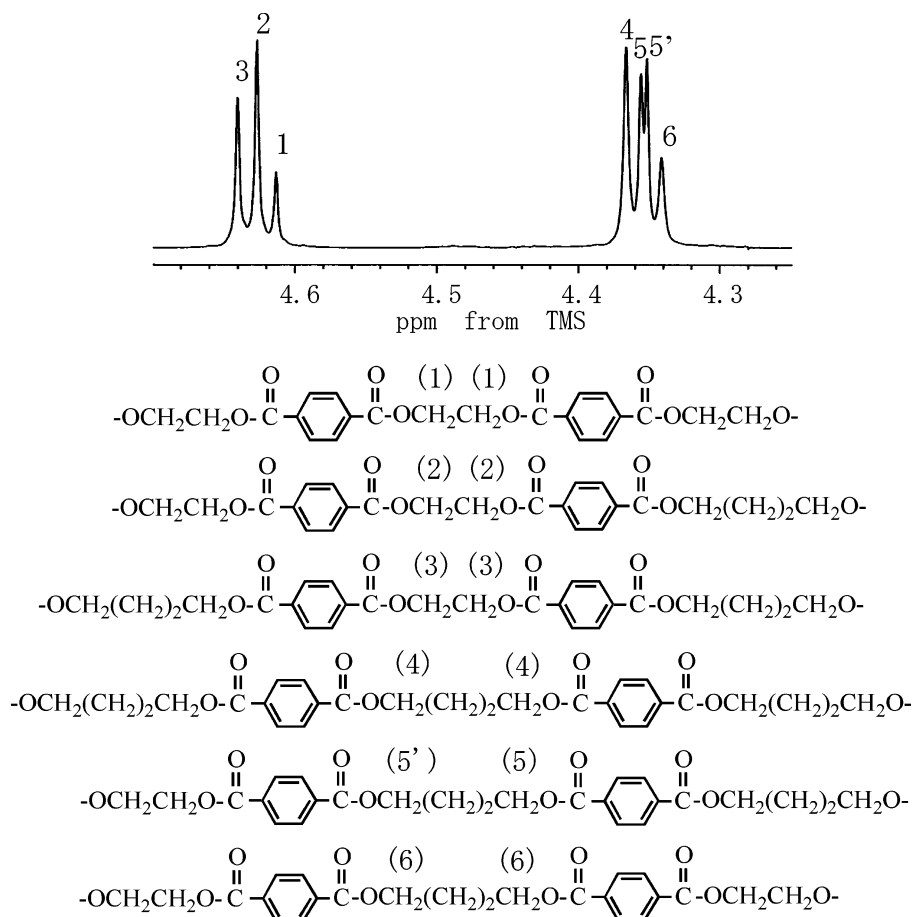


Figure 1. Expanded 600 MHz ^1H NMR spectra (the alcoholic CH_2 proton region) of poly(ethylene/butylene terephthalate) copolymers in 75/25 (v/v) mixture of *o*-chlorophenol/deuterated chloroform at 80 $^\circ\text{C}$ and the triad sequences on the glycol units together with the assignment.

Table 1. Triad Fractions Centered on Glycol Units and Number-Average Sequence Length in Poly(ethylene/butylene terephthalate) Copolymers^a

	reaction time (min)				
	10	30	60	90	120
EG-TA-EG-TA-EG	0.30	0.24	0.16	0.15	0.13
EG-TA-EG-TA-TMG	0.08	0.13	0.18	0.19	0.20
TMG-TA-EG-TA-TMG	0.01	0.02	0.05	0.06	0.08
EG-TA-TMG-TA-EG	0.52	0.44	0.38	0.33	0.30
EG-TA-TMG-TA-TMG	0.09	0.15	0.19	0.22	0.23
EG-TA-TMG-TA-EG	0.01	0.02	0.04	0.05	0.07
L_{PET}^b	8.4	4.6	2.7	2.6	2.3
L_{PBT}^c	11.7	6.4	4.4	3.7	3.3

^a Temperature of transesterification reaction, 300 $^\circ\text{C}$; PET/PBT = 40/60 mole ratio. ^b Number-average sequence length of PET segment determined by ^1H NMR. ^c Number-average sequence length of PBT segment determined by ^1H NMR.

It has been reported that the transesterification product between PET and PBT results in separate crystals of the two components rather than cocrystallization²⁹ because of faster crystallization of PBT than PET. Therefore, the above exclusion models can be applied to the PET/PBT copolymer. Figure 3 shows the correlation between the inverse of the melting temperature, $1/T_m$, and the natural logarithm of $X_A - 1/L$, $\ln(X_A - 1/L)$, in eq 2 for the transesterification products between PET and PBT at 300 $^\circ\text{C}$; the molar fractions are 0.39 and 0.61, respectively. Here, X_A is the molar fraction of the PBT unit, 0.61, and L is the number-average sequence length of the butylene terephthalate unit obtained by triad sequence analysis. The linear correlation between $1/T_m$ and $\ln(X_A - 1/L)$ was confirmed according to the eq 2. Therefore, although the

eq 2 proposed by Baur⁷ is expressed on a completely random copolymer, it was confirmed that this model can be applied to the PET/PBT block copolymers obtained by the transesterification reaction. The linear correlation in Figure 3 is considered because the copolyesters obtained by the transesterification reaction between PET and PBT can be regarded as the exclusion model and can give finally a completely random copolymer.⁵

On the other hand, the following relation between melting temperature and the lamellae thickness (Gibbs–Thomson equation) has been well-known:¹⁵

$$T_m = T_m^\circ - T_m^\circ (2\sigma_e / l \Delta H_m^\circ) \quad (3)$$

Here σ_e is the fold-surface free energy, ΔH_m° is the equilibrium heat of fusion/unit volume, and l is the

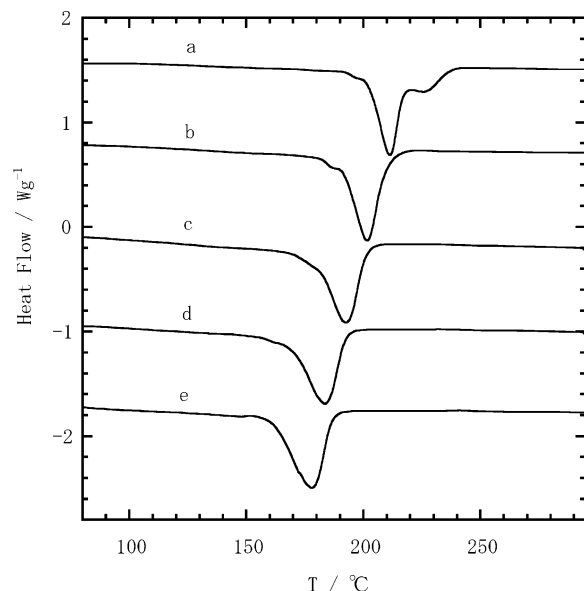


Figure 2. Differential scanning calorimeter curves of the transesterification products obtained by quench after the transesterification reaction between PET and PBT, 40 and 60 mol %, respectively, at 300 °C. The transesterification reaction time is (a) 10 min, (b) 30 min, (c) 60 min, (d) 90 min, and (e) 120 min.

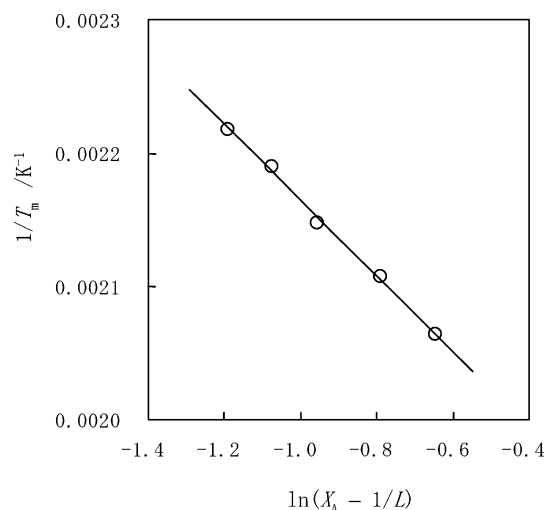


Figure 3. Relationship between the natural logarithm of $X_A - 1/L$, $\ln(X_A - 1/L)$, and the inverse of the melting temperature, $1/T_m$, of the transesterification products between PET and PBT, 40 and 60 mol %, respectively, where X_A indicates the molar fraction of the butylene glycol unit, 0.610, and L indicates the number-average sequence length of the butylene terephthalate unit.

Table 2. Melting Temperature and Long Period in Poly(ethylene/butylene terephthalate) Copolymers^a

	reacn time (min)				
	10	30	60	90	120
T_m (°C) ^b	211.5	201.5	192.8	183.6	177.9
long period (nm) ^c	13.8	13.3	12.2	11.0	11.0

^a Temperature of transesterification reaction, 300 °C; PET/PBT = 40/60 mole ratio. ^b Melting temperature determined by DSC. ^c Long period determined by SAXS.

lamellae thickness which is related to the apparent crystal size. l is usually measured by transmission electron microscopy (TEM), etc. In this paper, we attempted to apply the number-average sequence length L of butylene terephthalate or ethylene terephthalate

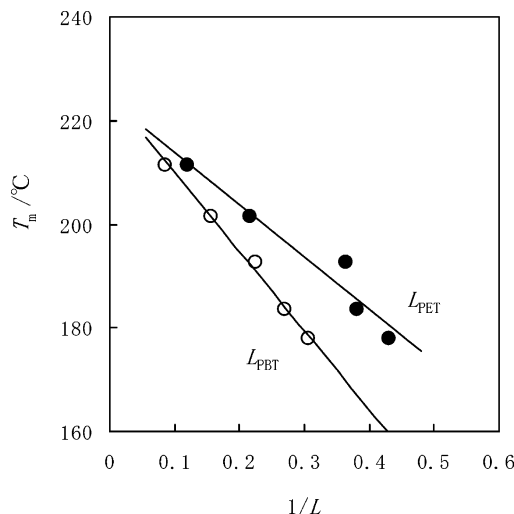


Figure 4. Relationship between the inverse of the number-average sequence length, $1/L$, and the melting temperature, T_m , of the transesterification products between PET and PBT, 40 and 60 mol %, respectively. L_{PET} and L_{PBT} indicate the number-average sequence lengths of the ethylene terephthalate and butylene terephthalate units, respectively.

unit determined by NMR instead of the lamellae thickness l in the Gibbs–Thomson equation. Consequently, the linear correlation between the melting temperature, T_m , and the inverse of the number-average sequence length, $1/L$, was observed as shown in Figure 4. In Figure 4, L_{PBT} and L_{PET} are the number-average sequence lengths of butylene terephthalate and ethylene terephthalate units, respectively. This linear correlation indicates that the number-average sequence length approximately corresponds to the lamellae thickness under the definite condition such as the quench after the transesterification. Thus, it was confirmed that the number-average sequence length, L , obtained by NMR can be approximately used instead of the lamellae thickness, l , in Gibbs–Thomson eq 3 on the melting temperature depression. To check this correlation, the analysis of the long period which reflects the crystal size of the transesterification product was performed using SAXS because the crystal size could not be estimated using wide-angle X-ray scattering due to the fine size and the low crystallinity.

Analysis Using SAXS. The scattered intensities and the mean long periods of the copolymers obtained by the transesterification reaction measured by SAXS decreased with increasing the transesterification reaction time as shown in Figure 5. These data mean the decrease of the crystal size with increasing the transesterification reaction time. The mean long periods were obtained from the tops of the peaks in Figure 5 as listed in Table 2. Figure 6 shows the relationship between the mean long period and the melting temperature of the copolymer obtained by quench after the transesterification reaction. The linear correlation was observed, and this seems to be reasonable because the melting temperature depends on the crystal size. On the other hand, the relationship between the inverse of the number-average sequence length of butylene terephthalate unit, $1/L_{PBT}$, and the mean long period of the transesterification products is shown in Figure 7. The linear correlation could be also shown. This indicates that the mean long period of the transesterification products depends on the number-average sequence length. The relationship between Figures 6 and 7 coincide with the

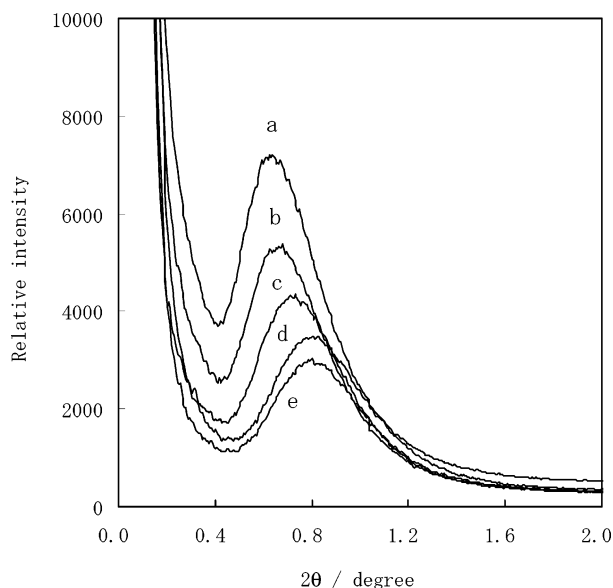


Figure 5. Small-angle X-ray scattering patterns of the transesterification products between PET and PBT, 40 and 60 mol %, respectively, at 300 °C. The transesterification reaction time is (a) 10 min, (b) 30 min, (c) 60 min, (d) 90 min, and (e) 120 min.

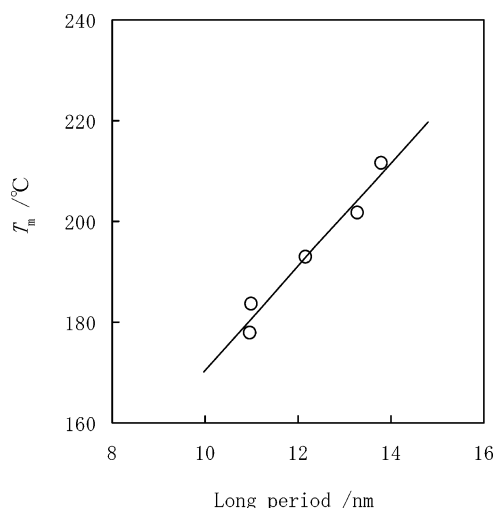


Figure 6. Relationship between the long period determined by SAXS and the melting temperature of the transesterification products between PET and PBT, 40 and 60 mol %, respectively.

linear correlation between the melting temperature and the inverse of the number-average sequence length in Figure 4. Thus, it was confirmed that the number-average sequence length, which is measured by NMR, of the transesterification product can be approximately used instead of the lamellae thickness in Gibbs–Thomson equation.

Analyses of Several Different Composition Samples. The relationships between the number-average sequence length and the melting temperature of the transesterification products were also investigated with different blend ratios of PET/PBT besides 40/60 mol % discussed above. The results are shown in Figure 8. The linear correlation between the inverse of the number-average sequence length of the butylene terephthalate unit and the melting temperature was observed for the transesterification products from 20/80 to 80/20 mol % of PET/PBT. Consequently, it was confirmed that the number-average sequence length can be approximately

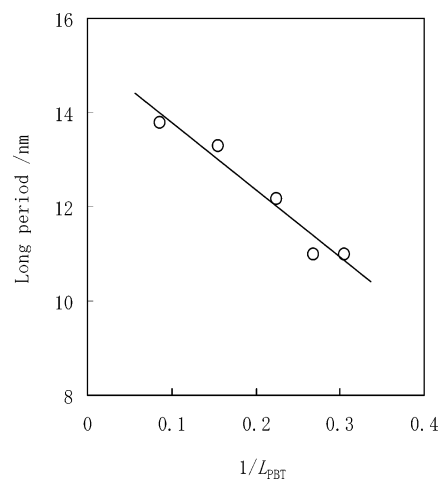


Figure 7. Relationship between the inverse of the number-average sequence length of butylene terephthalate unit, $1/L_{\text{PBT}}$, and the long period of the transesterification products between PET and PBT, 40 and 60 mol %, respectively.

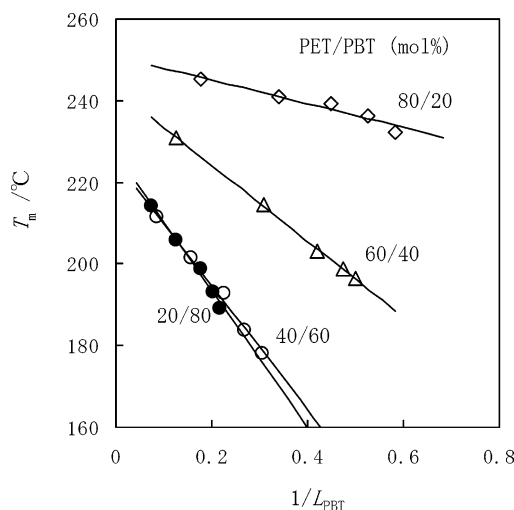


Figure 8. Relationship between the inverse of the number-average sequence length of the butylene terephthalate unit, $1/L_{\text{PBT}}$, and the melting temperature of the transesterification products between PET and PBT with composition of PET/PBT from 20/80 to 80/20 mol %.

used instead of the lamellae thickness in Gibbs–Thomson equation. This indicates that the tertiary structure, the lamellae thickness or crystalline size, of the transesterification products correlate with the primary structure, sequence distribution. As shown in Figure 8, the slope, that is, the degree of the melting temperature depression for the decrease of the number-average sequence length, increases with the increase of the composition of the butylene terephthalate unit. This is considered due to the larger rate of crystallization of the butylene terephthalate unit compared to the ethylene terephthalate unit. Thus, it was confirmed that the change of the sequence distribution of the butylene terephthalate unit in the transesterification reaction between PET and PBT gives a large influence for the melting temperature depression of the transesterification product.

Analysis Using High-Resolution Solid-State ¹³C NMR. To obtain the structural information on the transesterification products, high-resolution solid-state ¹³C NMR spectra were observed. Figure 9 shows 75.5 MHz CPMAS ¹³C NMR spectra of the transesterification product between PET and PBT, 40 and 60 mol %,

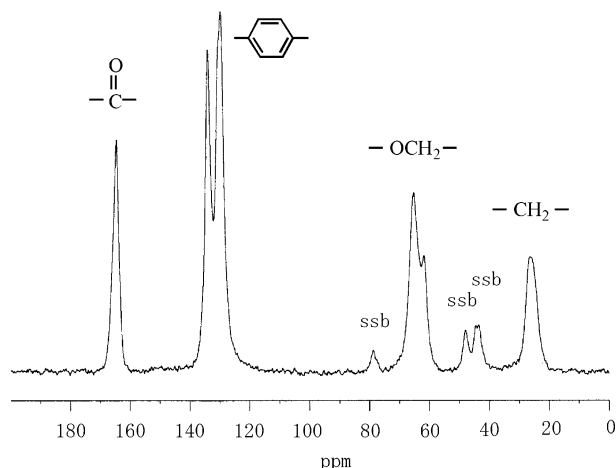


Figure 9. Solid-state ^{13}C NMR spectra (CPMAS) of the transesterification products between PET and PBT at 300 °C for 90 min, 40 and 60 mol %, respectively. The assignment is shown, and ssb means spinning sideband.

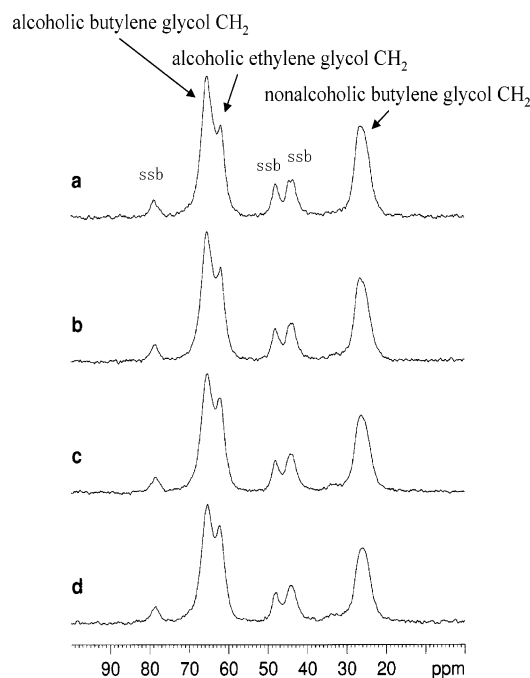


Figure 10. Expanded 75.5 MHz solid-state ^{13}C NMR spectra (CPMAS) (the glycol CH_2 carbon region) of the transesterification product between PET and PBT, 40 and 60 mol %, respectively, at 300 °C. The transesterification reaction time is (a) 10 min, (b) 30 min, (c) 60 min, and (d) 90 min.

respectively. The solid-state NMR spectrum includes the information on the crystalline and amorphous parts. Figure 10 shows the expanded glycol carbon peaks of several transesterification products between PET and PBT, 40 and 60 mol %, respectively. The decrease of the relative peak area of the alcoholic and nonalcoholic methylene carbon of the butylene glycol unit was observed as the progress of the transesterification. The relationship between the long period determined by SAXS and the ratio of the relative peak area of the methylene carbon of the butylene glycol (alcoholic or nonalcoholic methylene carbon) and ethylene glycol (alcoholic methylene carbon) units, $I_{\text{PBT}}/I_{\text{PET}}$, is shown in Figure 11. The decrease of $I_{\text{PBT}}/I_{\text{PET}}$ with the decrease of the long period as the progress of the transesterification was confirmed. As mentioned above, the crystalline size decreases as the progress of the transesterifi-

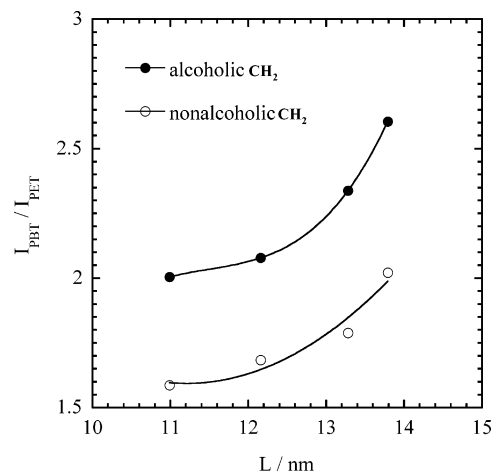


Figure 11. Relationship between the long period and the ratio of the relative peak area of the CH_2 carbon of the butylene glycol and ethylene glycol units, $I_{\text{PBT}}/I_{\text{PET}}$, of the transesterification products between PET and PBT, 40 and 60 mol %, respectively, at 300 °C. I_{PBT} and I_{PET} indicate the peak area of the CH_2 carbon (alcoholic and nonalcoholic CH_2 carbon) of the butylene glycol and ethylene glycol units, respectively.

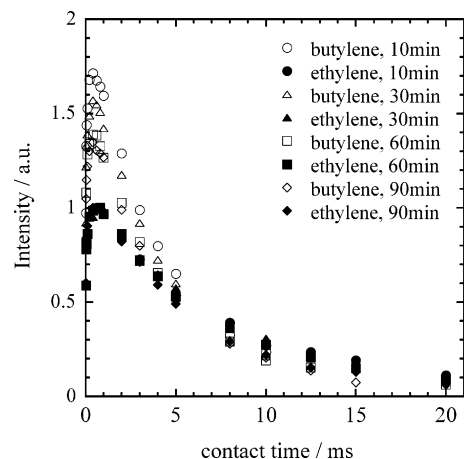


Figure 12. Contact time dependence of ^{13}C intensities of butylenes glycol (open) and ethylene glycol (closed) units in CPMAS experiment at room temperature for each transesterification product between PET and PBT, 40 and 60 mol %, respectively, at 300 °C.

cation. On the other hand, the densities of the transesterification products measured by density gradient column were nearly equal (1.326, 1.337, 1.341, 1.340, and 1.333 for 10, 30, 60, 90, and 120 min of the transesterification reaction time at 300 °C, respectively). So, the change of the crystallinity by transesterification can be almost negligible. Therefore, the decrease of the ratio of the relative peak area of the methylene carbon of the butylene glycol (alcoholic or nonalcoholic methylene carbon) and ethylene glycol (alcoholic methylene carbon) units, $I_{\text{PBT}}/I_{\text{PET}}$, in the solid-state ^{13}C NMR spectra as the progress of the transesterification is considered to be the result of the decrease of the crystalline size rather than the change in the crystallinity. As shown in Figure 12, the same behavior was recognized in the maximum intensity (relative) of the ^{13}C signals for various contact times in CPMAS experiment of each transesterification product. Such a phenomenon can be interpreted by the change in the local motion of each group with the decrease in size of the each domain as the progress of the transesterification.³⁰

Conclusion

The relationship between the number-average sequence length and the melting temperature of the block copolyesters obtained by quench after the transesterification reaction between PET and PBT was investigated. The linear correlation between the inverse of the number-average sequence length and the melting temperature was observed for the transesterification products with composition of PET/PBT from 20/80 to 80/20 mol %. This correlation was confirmed by the correlation between the long period determined by small-angle X-ray scattering and the number-average sequence length and between the long period and the melting temperature. For the transesterification products, it was confirmed that the number-average sequence length measured by NMR can be approximately used instead of the lamellae thickness in Gibbs–Thomson equation that has been well-known as the relationship between the melting temperature and the lamellae thickness. The decrease of the ratio of the relative peak area of the methylene carbon of the butylene glycol and ethylene glycol units, $I_{\text{PBT}}/I_{\text{PET}}$, in the solid-state ^{13}C NMR spectra was observed as the progress of the transesterification. It was considered to be the result of the change in the local motion of each segment reflecting the decrease of the crystalline size.

Acknowledgment. The authors thank Mr. Hirofumi Kurimoto at Teijin Ltd. for his support of the small-angle X-ray scattering measurements.

References and Notes

- (1) Bovey, F. A. *High-Resolution NMR of Macromolecules*; Academic Press: New York, 1972.
- (2) Matsuzaki, K.; Uryu, T.; Asakura, T. *NMR Spectroscopy and Stereoregularity of Polymers*; Japan Scientific Societies Press: Tokyo, 1996.
- (3) Herbert, I. R. Statistical analysis of copolymer sequence distribution. In *NMR Spectroscopy of Polymers*; Ibbett, R. N., Ed.; Blackie Academic & Professional: Glasgow, U.K., 1993.
- (4) Fakirov, S. *Transreactions in Condensation Polymers*; Wiley-VCH: Weinheim, Germany, 1999.
- (5) Matsuda, H.; Asakura, T.; Miki, T. *Macromolecules* **2002**, *35*, 4664.
- (6) Flory, P. J. *Trans. Faraday Soc.* **1955**, *51*, 848.
- (7) Baur, V. H. *Makromol. Chem.* **1966**, *98*, 297.
- (8) Sanchez, I. C.; Eby, R. K. *Macromolecules* **1975**, *8*, 638.
- (9) Helfand, E.; Lauritzen, J. I. *Macromolecules* **1973**, *6*, 631.
- (10) Dole, M.; Wunderlich, B. *Makromol. Chem.* **1959**, *34*, 29.
- (11) Goulet, L.; Prud'Homme, R. E. *J. Polym. Sci., Polym. Phys. Ed.* **1990**, *28*, 2329.
- (12) Allegra, G.; Marchessault, R. H.; Bloembergen, S. *J. Polym. Sci., Polym. Phys. Ed.* **1992**, *30*, 809.
- (13) Goldbeck-Wood, G. *Polymer* **1992**, *33*, 778.
- (14) Kamiya, N.; Sakurai, M.; Inoue, Y.; Chujo, R. *Macromolecules* **1991**, *24*, 3888.
- (15) Hoffman, J. D.; Weeks, J. J. *J. Chem. Phys.* **1962**, *37*, 1723.
- (16) Weimann, P. A.; Hajduk, D. A.; Chaffin, K. A.; Brodil, J. C.; Bates, F. S. *J. Polym. Sci., Polym. Phys. Ed.* **1999**, *37*, 2053.
- (17) Xie, X. L.; Fung, K. L.; Li, R. K. Y.; Tjong, S. C. Mai, Y. W. *J. Polym. Sci., Polym. Phys. Ed.* **2002**, *40*, 1214.
- (18) Ha, W. S.; Chun, Y. K.; Jang, S. S.; Rhee, D. M.; Park, C. R. *J. Polym. Sci., Polym. Phys. Ed.* **1997**, *35*, 309.
- (19) Hamb, F. L. *J. Polym. Sci., Polym. Chem. Ed.* **1972**, *10*, 3217.
- (20) Misra, A.; Garg, S. N. *J. Polym. Sci., Polym. Phys. Ed.* **1986**, *24*, 983.
- (21) Kamiya, N.; Yamamoto, Y.; Inoue, Y.; Chujo, R.; Doi, Y. *Macromolecules* **1989**, *22*, 1676.
- (22) Yoo, H. Y.; Umemoto, S.; Kikutani, T.; Okui, N. *Polymer* **1994**, *35*, 117.
- (23) Kiyotsukuri, T.; Masuda, T.; Tsutsumi, N. *Polymer* **1994**, *35*, 1274.
- (24) Li, B.; Yu, J.; Lee, S.; Ree, M. *Polymer* **1999**, *40*, 5371.
- (25) Li, B.; Yu, J.; Lee, S.; Ree, M. *Eur. Polym. J.* **1999**, *35*, 1607.
- (26) Lee, S. W.; Ree, M.; Park, C. E.; Jung, Y. K.; Park, C. S.; Jin, Y. S.; Bae, D. C. *Polymer* **1999**, *40*, 7137.
- (27) Karayannidis, G. P.; Sideridou, I. D.; Zamboulis, D. N.; Bikiaris, D. N. *J. Appl. Polym. Sci.* **2000**, *78*, 200.
- (28) Jeong, Y. G.; Jo, W. H.; Lee, S. C. *Macromolecules* **2003**, *36*, 4051.
- (29) Escala, A.; Stein, R. S. *Adv. Chem. Ser.* **1979**, No. 176, 455.
- (30) Schulze, D.; Ernst, H.; Fenzke, D.; Meiler, W.; Pfeifer, H. *J. Phys. Chem.* **1990**, *94*, 3499.

MA049490W